Supporting Information

Synthesis and Characterization of Sequence-controlled Semicrystalline Comb Copolymers: Influence of Primary Structure on Materials Properties

*Sansanee Srichan, Navaphun Kayunkid, Laurence Oswald, Bernard Lotz, and Jean-François Lutz**

Institut Charles Sadron, UPR22-CNRS, 23 rue du Loess, BP84047

67034 Strasbourg Cedex 2, France.

E-mail: jflutz@unistra.fr

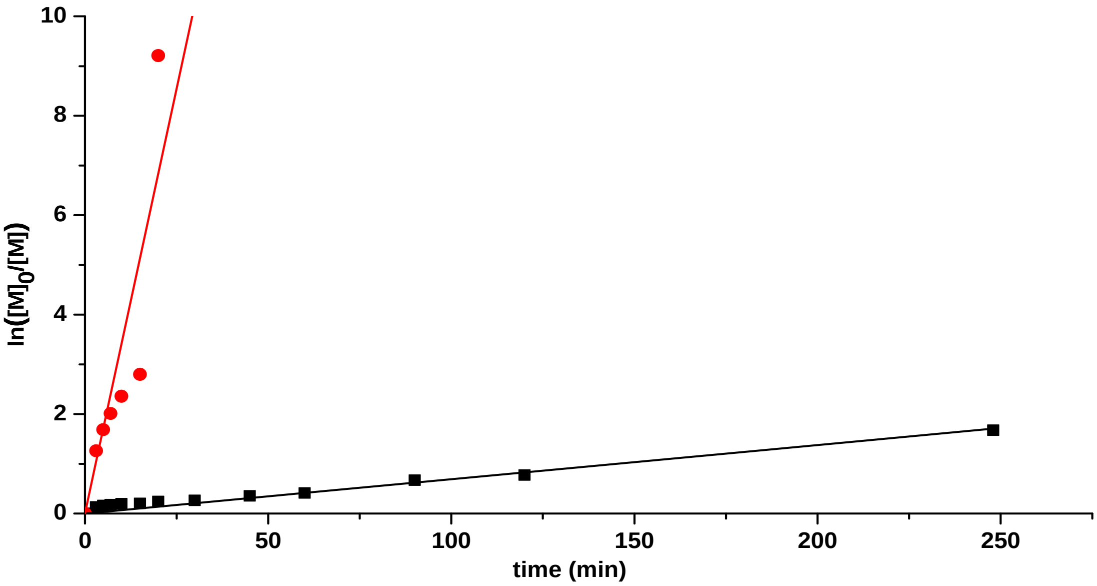

Figure S1. Semi-logarithmic plot of monomer conversion versus time recorded for the sequence-controlled copolymerization of **1** and **2** (copolymer **C1** in Table 2).

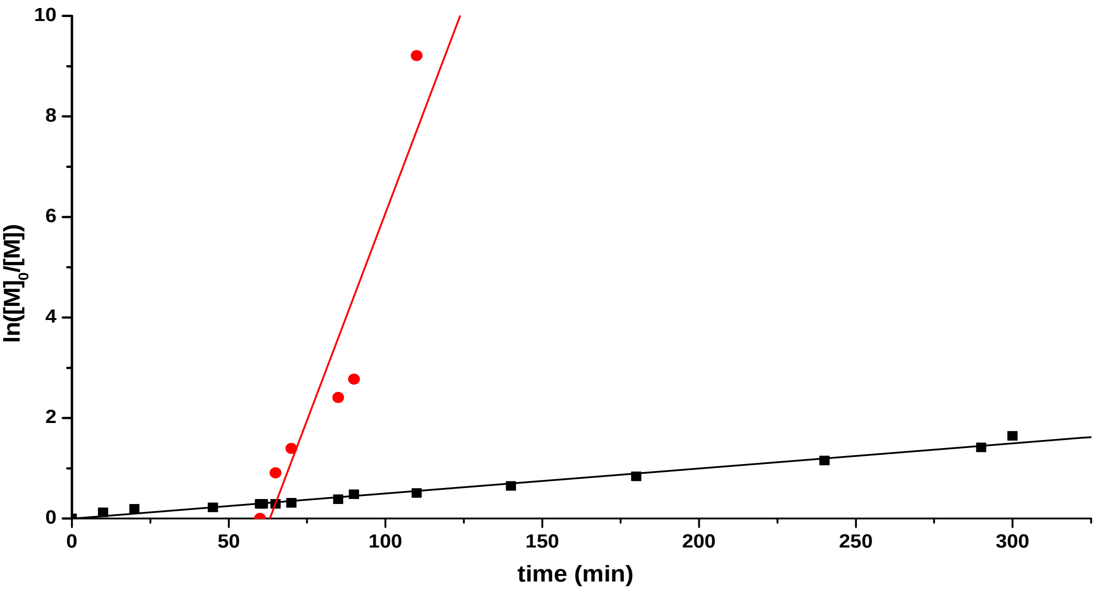

Figure S2. Semi-logarithmic plot of monomer conversion versus time recorded for the sequence-controlled copolymerization of **1** and **2** (copolymer **C2** in Table 2).

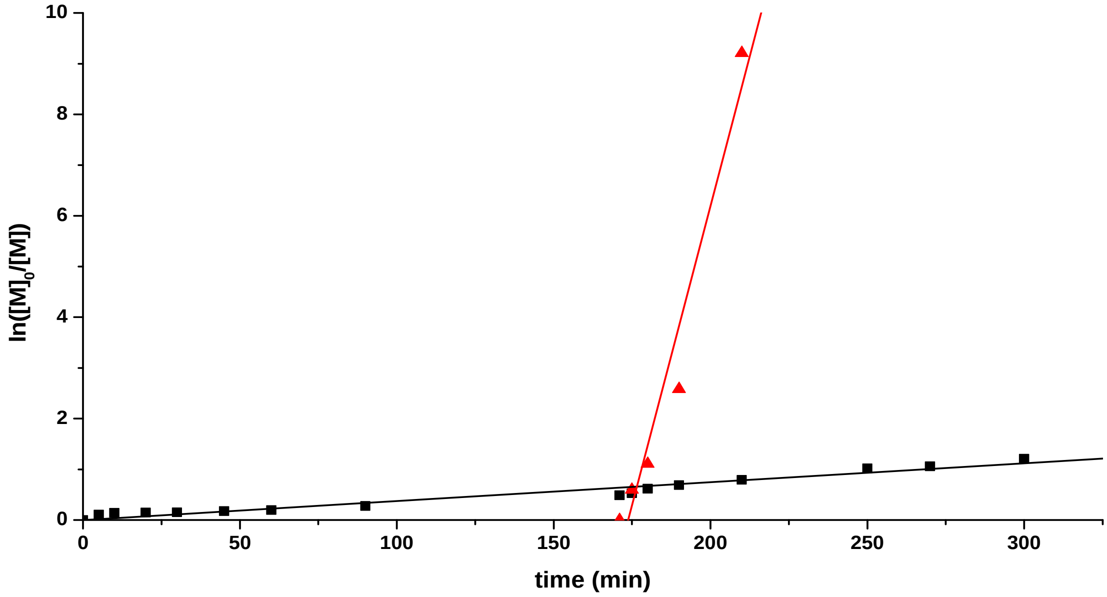

Figure S3. Semi-logarithmic plot of monomer conversion versus time recorded for the sequence-controlled copolymerization of **1** and **3** (copolymer **C6** in Table 2).

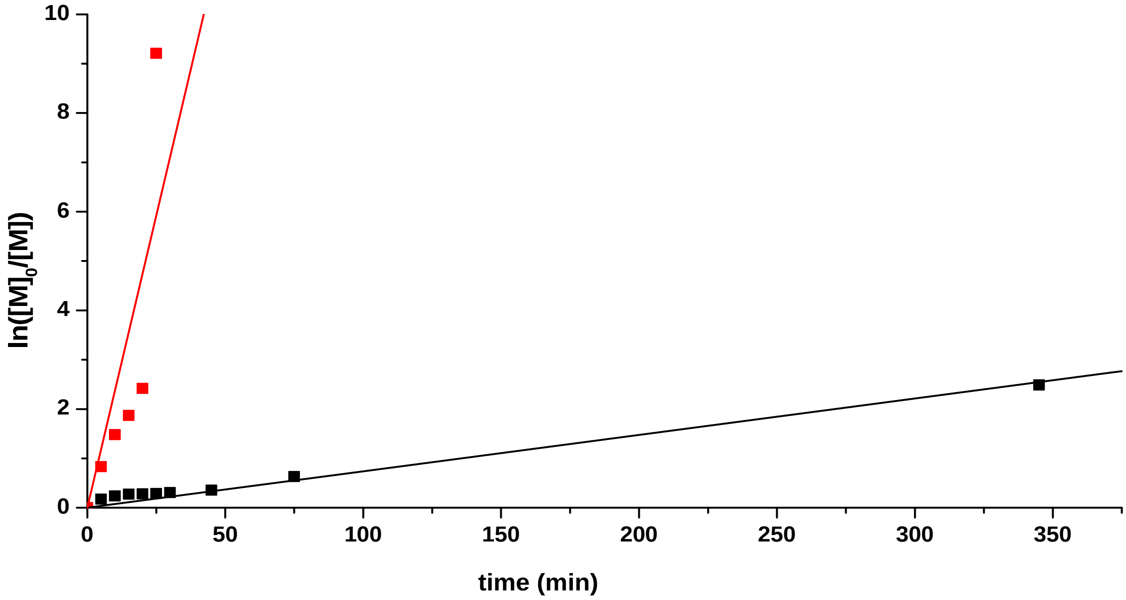

Figure S4. Semi-logarithmic plot of monomer conversion versus time recorded for the sequence-controlled copolymerization of **1** and **4** (copolymer **C7** in Table 2).

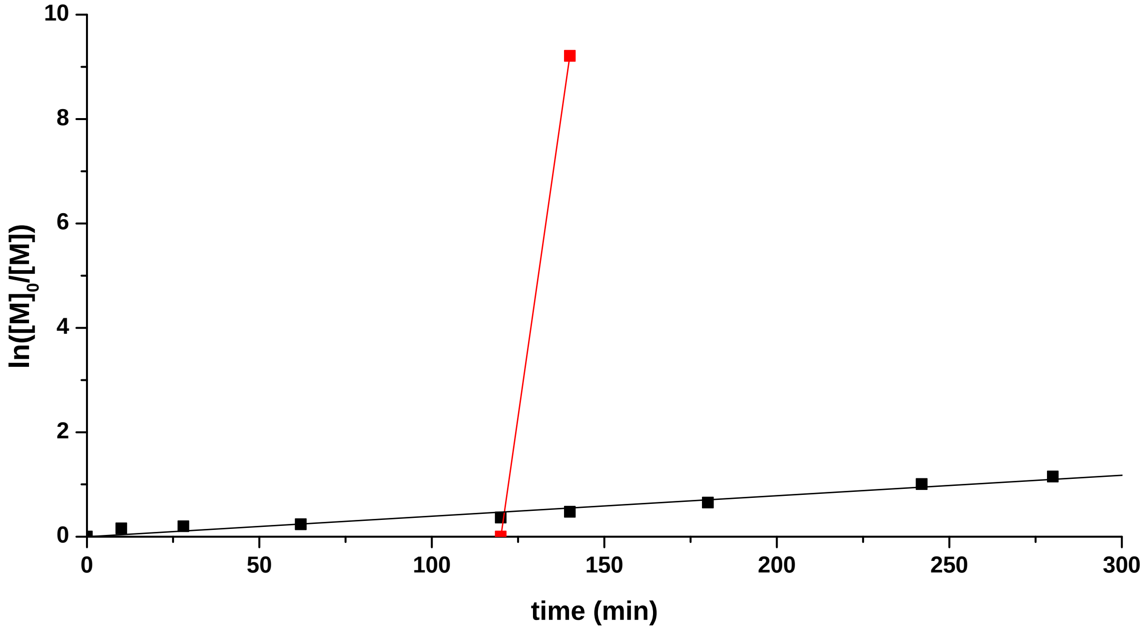

Figure S5. Semi-logarithmic plot of monomer conversion versus time recorded for the sequence-controlled copolymerization of **1** and **4** (copolymer **C9** in Table 2).

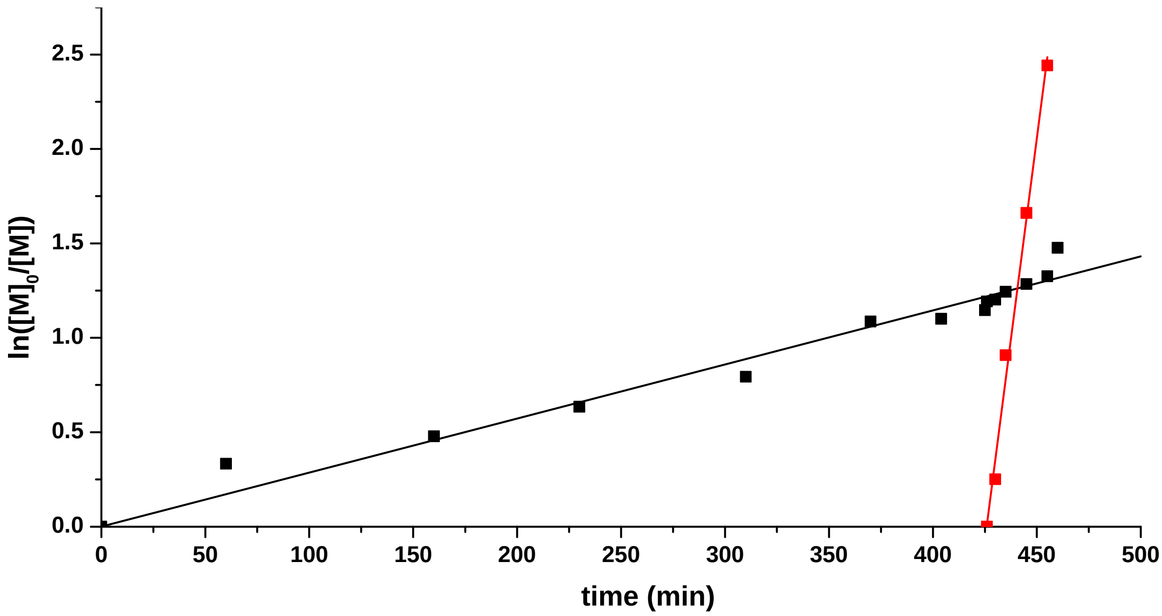

Figure S6. Semi-logarithmic plot of monomer conversion versus time recorded for the sequence-controlled copolymerization of **1** and **4** (copolymer **C11** in Table 2).

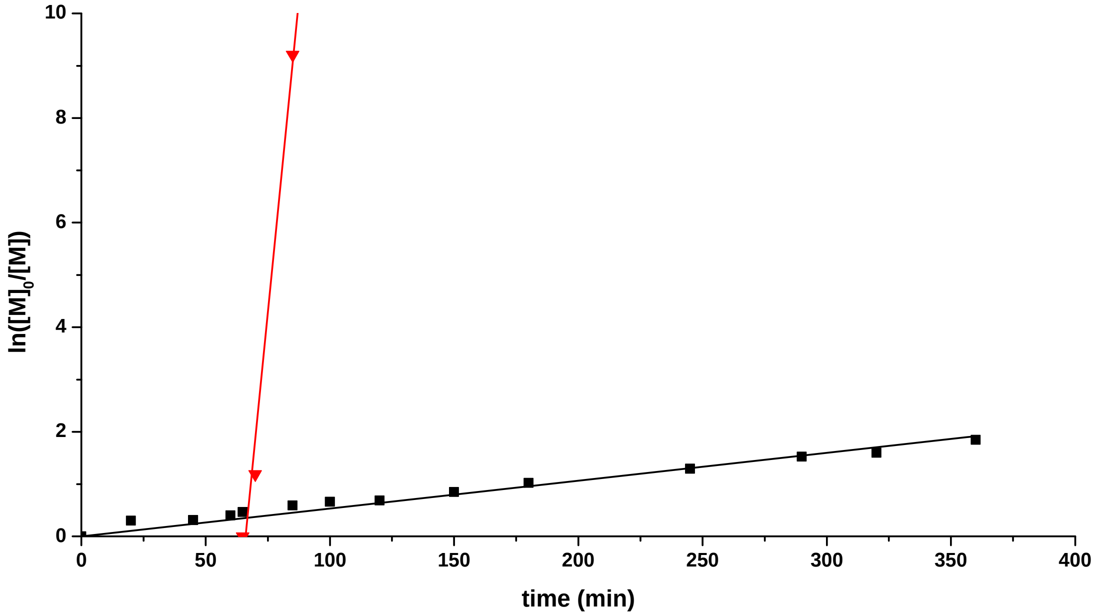

Figure S7. Semi-logarithmic plot of monomer conversion versus time recorded for the sequence-controlled copolymerization of **1** and **5** (copolymer **C13** in Table 2).

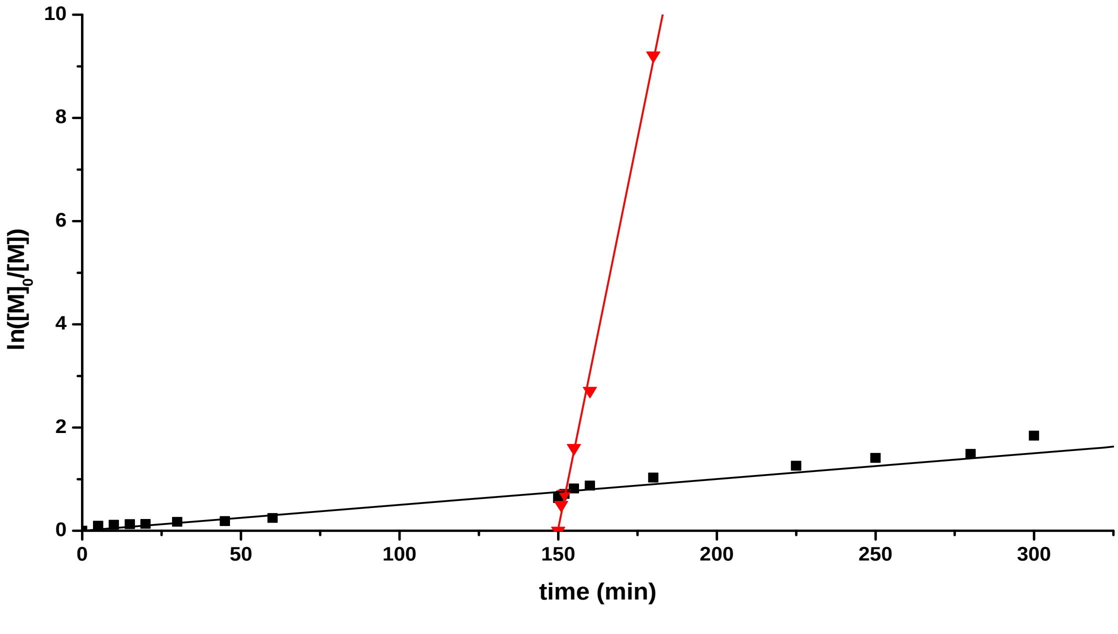

Figure S8. Semi-logarithmic plot of monomer conversion versus time recorded for the sequence-controlled copolymerization of **1** and **5** (copolymer **C14** in Table 2).

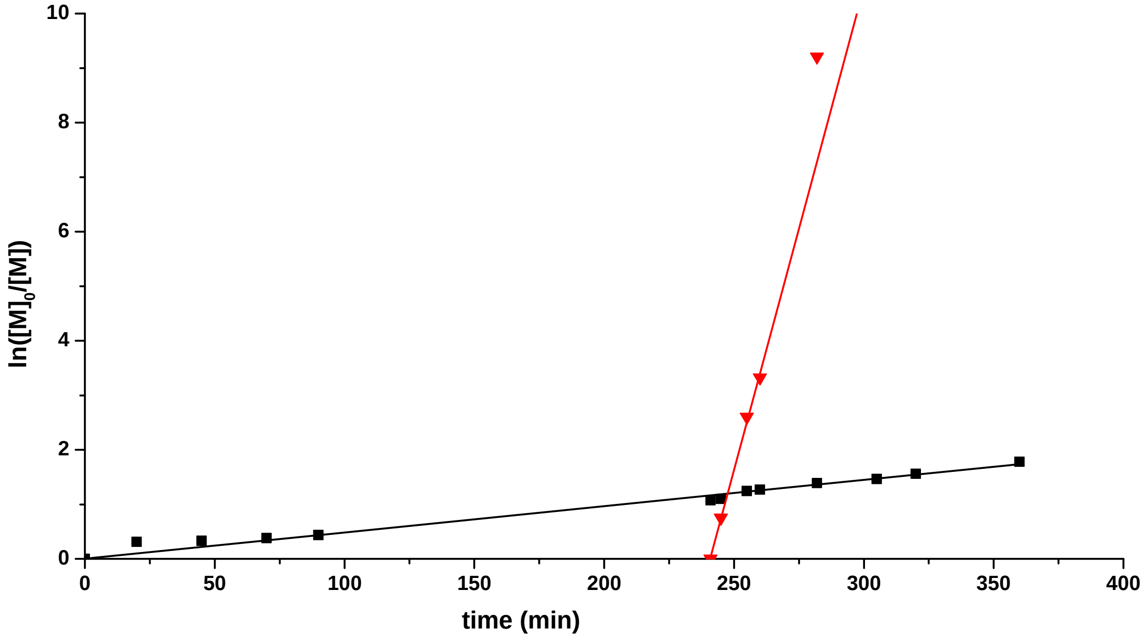

Figure S9. Semi-logarithmic plot of monomer conversion versus time recorded for the sequence-controlled copolymerization of **1** and **5** (copolymer **C15** in Table 2).

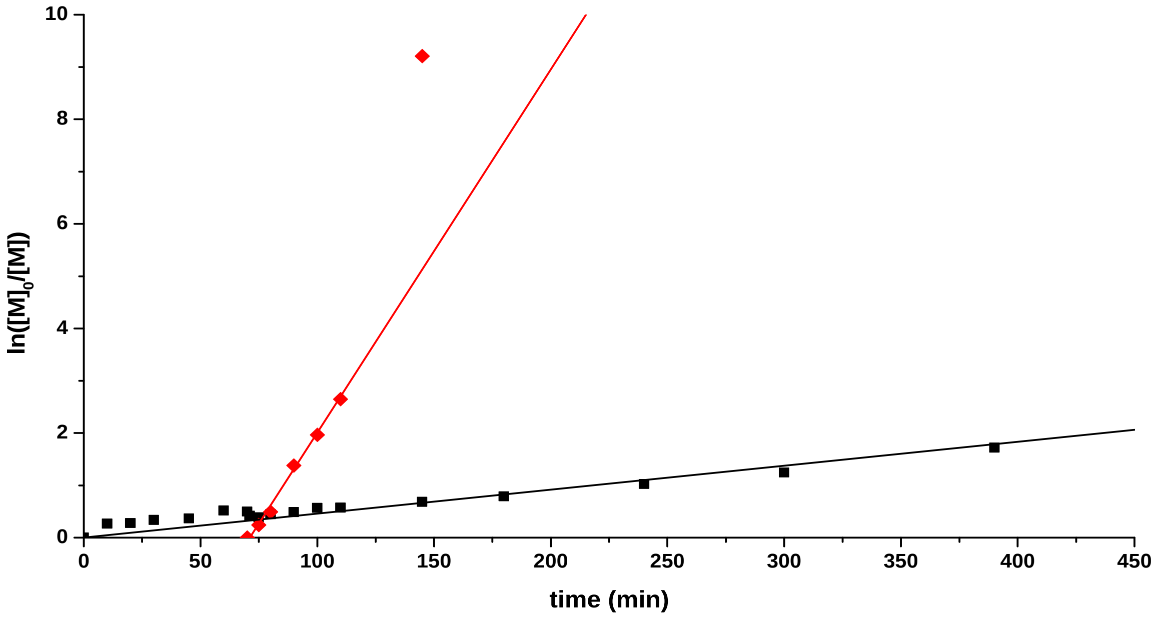

Figure S10. Semi-logarithmic plot of monomer conversion versus time recorded for the sequence-controlled copolymerization of **1** and **6** (copolymer **C16** in Table 2).

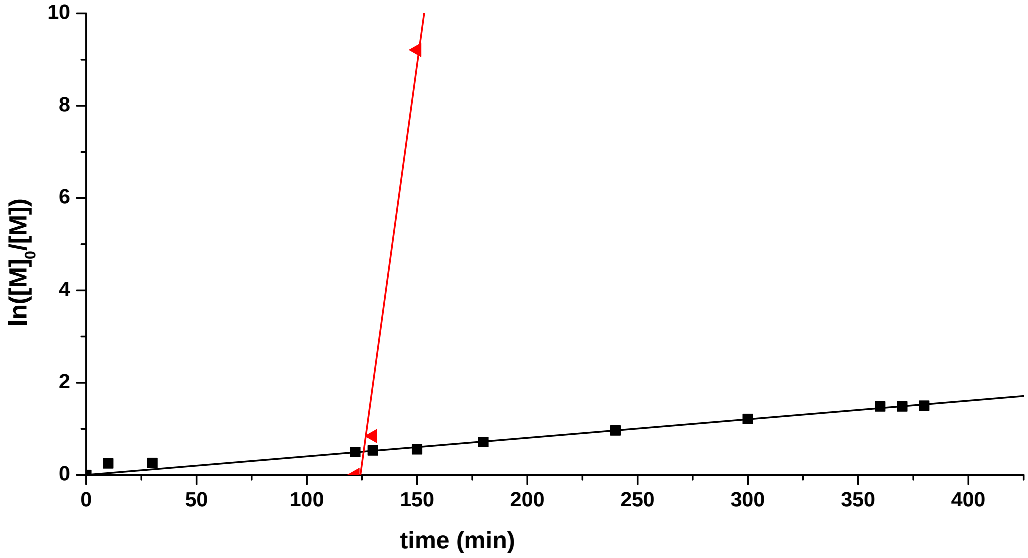

Figure S11. Semi-logarithmic plot of monomer conversion versus time recorded for the sequence-controlled copolymerization of **1** and **7** (copolymer **C17** in Table 2).

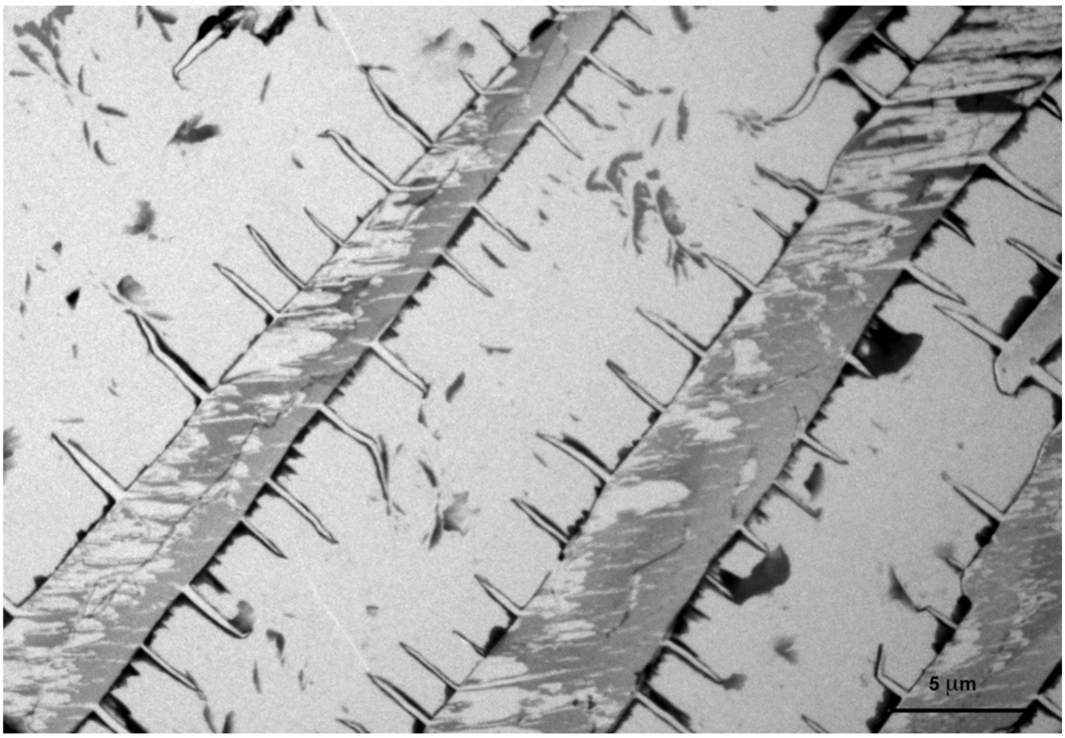

Figure S12. Bright field image of the epitaxial crystallization of copolymer **C2**. The diagonal areas are the traces of benzoic acid crystals that have grown in and over a thin layer of copolymer **C2**. On cooling, **C2** crystallizes epitaxially on the surface of the benzoic acid. After dissolution of the acid, the oblique dark grey domains of **C2** are clearly visible. They are made of stacks of edge-on lamellae. Note the orientation of these stacks, nearly horizontal in this picture i.e. in proper relative orientation to the diffraction patterns below.

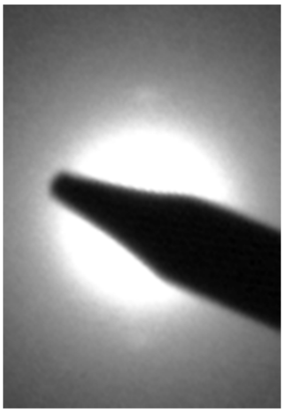

Figure S13. The central part of the diffraction pattern (here taken with a longer camera length) helps visualize the diffraction peaks due to the stacked lamellae. The periodicity of the lamellar thickness L is here 53 Å. Only the second and third order diffractions are visible as in Figure 3b.

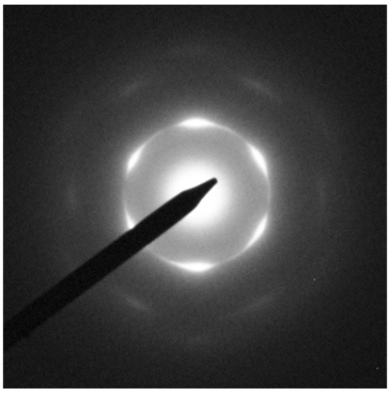

Figure S14. In areas with no benzoic acid, the thin films crystallize with the lamellar structure parallel to the support. The chain axes are here normal to the sheet. The packing is hexagonal. The first ring of reflections corresponds to the 100 spots, spacing 4.15 Å. The second ring corresponds to 110 reflections.

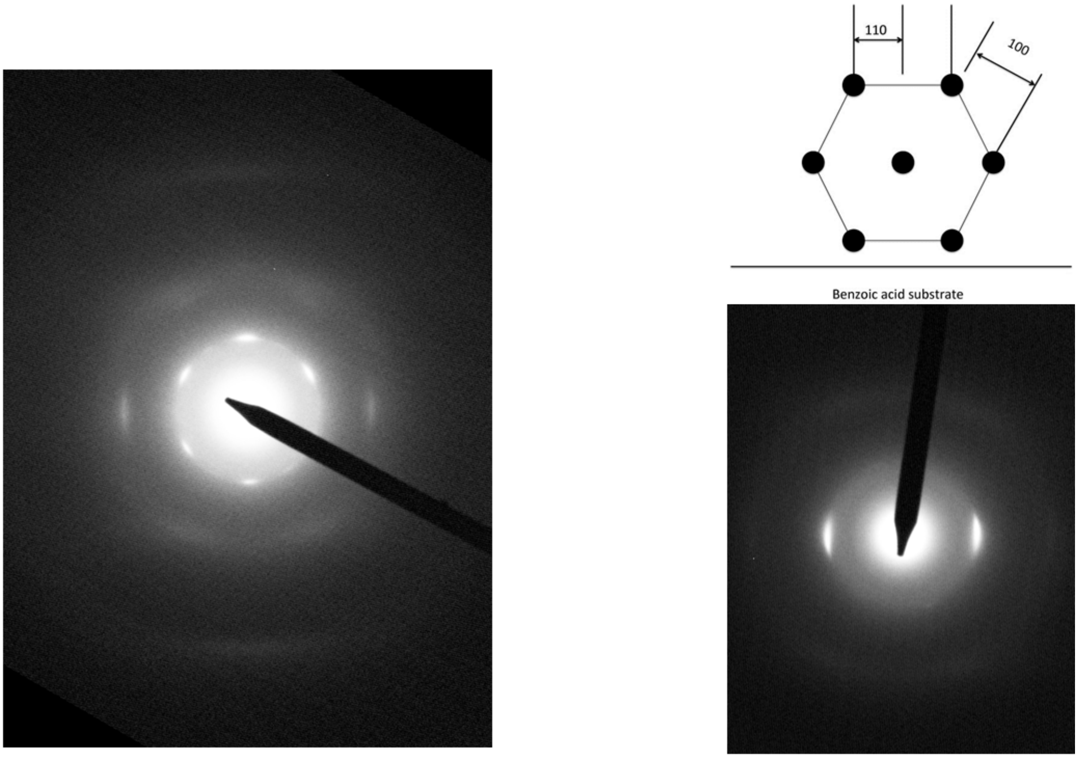

Figure S15. Left: This diffraction pattern of sample **C2** was taken from an area where epitaxial crystallization took place. This pattern is "spoiled" by diffraction from a nearby single crystal as in Figure S14: the inner rings of 100 reflections are due to the single crystal and are not part of the epitaxially crystallized material. The feature of interest in the epitaxial part of the pattern is the fact that no 100 reflection is apparent on the equator. Only the outer 110 reflection is present. This indicates that the contact plane is the densely packed 100 plane of the aliphatic segments. The interchain distance in this plane is ≈5 Å which nearly matches the a parameter of benzoic acid (5.2 Å). In order to see the strong 100 spot of the epitaxially crystallized film, one needs to rotate the sample along the vertical chain axis by 30°. This is shown in the figure at the right. Epitaxial crystallization thus makes it possible to generate a multilayered of multilamellar structure that is nevertheless single crystalline since each lamella interacts in the same way with a common single crystalline substrate.